Uchida, Tatsuhiko; Kawahara, Yoshihisa

Optimal Interpolation of Submerged River Bed for Laser Scanning Survey Using a Two-Dimensional Numerical Model

OPTIMAL INTERPOLATION OF SUBMERGED RIVER BED FOR LASER SCANNING SURVEY USING A TWO-DIMENSIONAL NUMERICAL MODEL

Tatsuhiko[1] Uchida and Yoshihisa Kawahara[2]

[1] Associate Professor, Research and Development Initiative, Chuo University,
1-13-27, Kasuga, Bunkyo-ku, Tokyo, 112-8551, Japan, e-mail: utida@tamacc.chuo-u.ac.jp
[2] Professor, Department of Civil and Environmental Engineering, Hiroshima University,
1-4-1, Kagamiyama, Higashi-Hiroshima, 739-8527, Japan, e-mail: kawahr@hiroshima-u.ac.jp

ABSTRACT

LiDAR (laser-induced direction and ranging) mounted on an airborne has been developed and used to measure the physical environment of rivers. However, it is still very difficult to obtain submerged river bed topography because of the presence of fluctuating water surface and weakly-laser-transmission of river water. This paper proposes a new and practical method to interpolate the submerged bed shape by water surface profiles in compensation for the weak points of LiDAR.

First, we survey the complex bed topography of an experimental channel in details by terrestrial LiDAR. To discuss the feasibility to interpolate river bed profile from known water surface profile, we conduct numerical simulations of flows for various bed topographies by the shallow water model. This resulted that the least error of water surface leads to the least error of submerged bed topography. Then, we formulate the algorithm of a new hydrodynamic interpolation method to estimate the optimal submerged river bed topography using water surface profile. It is confirmed that the hydrodynamic interpolation can modify submerged river bed topography toward the measured one. Because longitudinal water level profiles can be obtained by LiDAR, the present method may be a powerful technique to interpolate the submerged bed topography in compensation for the weak point of LiDAR.

Keywords: laser scanner, digital terrain model, submerged river bed topography, water surface, hydrodynamic interpolation method, shallow water numerical model, CIP scheme

1. INTRODUCTION

Recently airborne LiDAR (laser-induced direction and ranging) has been developed and used to measure the physical environment of rivers. It provides laser-based measurements of the distance between the sensor on an aircraft and the object. LiDAR has many advantages. The resulting measurements have high precision and can be post-processed to an accurate digital terrain model. Uchida *et al.* (2007) demonstrated that LiDAR mounted on a helicopter has potentials to detect longitudinal profiles of water edge and mean diameter of surface gravels. On the other hand, it has the limitation to detect river bed under thick vegetation or water surface. Especially, it is still very difficult to obtain submerged river bed topography because of the presence of fluctuating water surface and weakly-laser-transmission of river water. The examination of submerged river bed topography is important to estimate the amount of sediment transport in flood events.

Actually, water surface profiles are controlled by discharge, bed roughness and bed profiles. This means that a water surface profile may be a guide for us to estimate the bed topography with reasonable magnitude of errors, if the discharge and bed roughness are known. This paper proposes a new practical method to interpolate the submerged bed shape by using a water surface profile and a shallow-water model in compensation for the weak point of LiDAR.

First, we survey the complex bed topography of an experimental channel in details by terrestrial LiDAR. A geometric interpolation method, which solves the Laplace equations for bed elevation and its gradient along water edges, is applied to the bed profile submerged by a low-flow in the experimental channel. Then, we conduct numerical simulations of flows for various bed topographies, which are interpolated by the geometric method, by the shallow water model (Uchida, 2006) to discuss the feasibility to interpolate river bed profile from known water surface profile. Then we formulate the algorithm of a new hydrodynamic interpolation method to estimate the optimal submerged river bed topography using water surface profile.

2. MEASUREMENT OF COMPARATIVE SUBMERGED BED TOPOGRAPHY AND ITS GEOMETRIC INTERPOLATION METHOD

To develop an estimation method, detail and accurate data of submerged river bed is necessary. We survey the complex bed topography of an experimental channel in details by terrestrial LiDAR (Leica Geosystems), because it is very difficult to obtain submersible bed profiles of rivers. Figure 1 (a) shows 3D spatial data of dry bed topography formed by water flow in the experimental channel of 10m length and 1.5m width. The surface of sand bed was packed by adhesion bonds. We also obtain the data with water flow ($Q=3.5 *10^{-3}m^3$). Then,

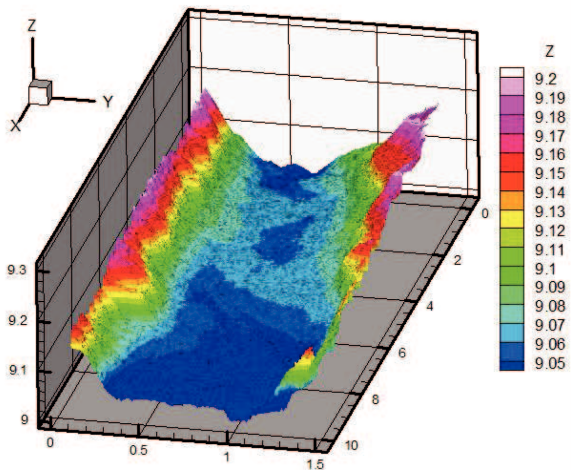

(a) 3D spatial data of bed topography

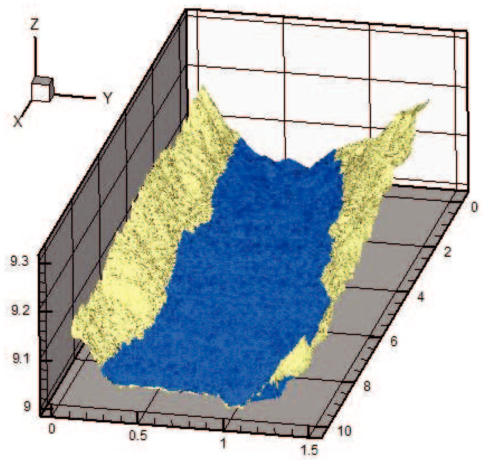

(b) Wet and dry region
Blue: wet region, Yellow: dry region

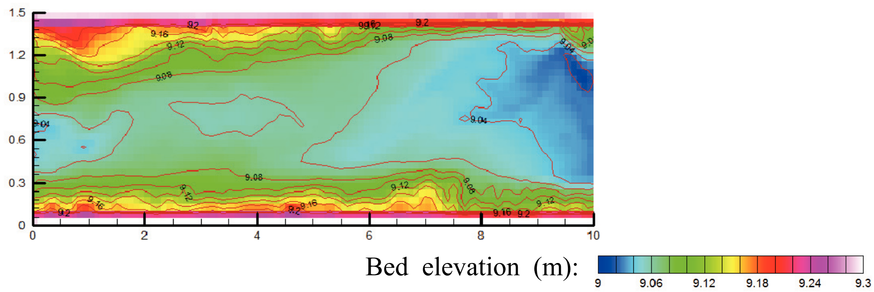

(c) Comparative bed profile of mesh data (dx=0.10m, dy=0.05m)

Figure 1 3D spatial data of bed topography and mesh data we separate the data into wet and dry region, as shown in Figure 1 (b). The comparative bed profile of mesh data (dx=0.10m, dy=0.05m) is generated by LiDAR data of Figure 1 (a), as shown in Figure 1 (c).

To develop a hydrodynamic interpolation method of submerged bed profile, the geometric interpolation method with Laplace equations is applied. In this paper, submerged bed topography z_w is represented by Eq. 1.

$$z_w = z_0 + \alpha(z_1 - z_0) \tag{1}$$

in which, α is defined by correction coefficient of water depth in this paper. z_0 and z_1 are solutions of the Laplace equations for bed elevation and its gradient along water edges, respectively. Those solutions are obtained by Eq. 2 and 3.

$$\nabla^2 z_0 = 0 \tag{2}$$

$$\nabla^2(\partial z_1 / \partial x) = \nabla^2 z_{1x} = 0, \quad \nabla^2(\partial z_1 / \partial y) = \nabla^2 z_{1y} = 0 \tag{3}$$

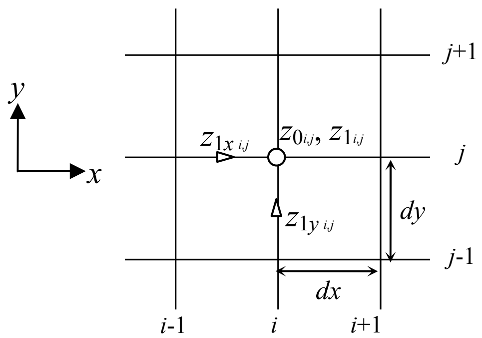

Figure 2 Arrangements of variables to compute Laplace equations of bed level slopes

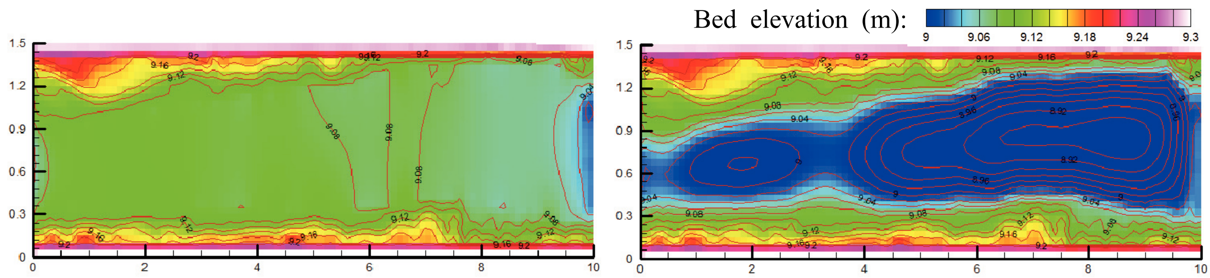

(a) z_0 by Laplace equation of bed level (b) z_1 by Laplace equations of bed level slopes

Figure 3 Interpolated bed profiles by Laplace equations of bed level and its gradients

To compute bed levels by Laplace equations of its gradient x,y of Eq. 3, variables at i, j are disposed as shown in Figure 2. Bed levels $z_{1i,j}$ by Laplace equations of its gradient are obtained by a iterative computation of Eq. 4 with solutions of Eq. 3.

$$z_{1\,i,j} = \frac{1}{4}\left(z_{1\,i-1,j} + z_{1x\,i,j} \cdot dx\right) + \frac{1}{4}\left(z_{1\,i+1,j} - z_{1x\,i+1,j} \cdot dx\right) + \frac{1}{4}\left(z_{1\,i,j-1} + z_{1y\,i,j} \cdot dy\right) + \frac{1}{4}\left(z_{1\,i,j+1} - z_{1y\,i,j+1} \cdot dy\right) \tag{4}$$

Figure 3 (a) and (b) show interpolated bed profiles by Laplace equations of bed level and its gradients, respectively. The submerged bed level interpolated by Eq. 2 is higher than the real value of Figure 2 at any point, because it should be understood that the submerged bed level is under than that of the dry area. That is, the solution z_0 by Eq. 2 is considered as the submerged bed level with zero water depth. In contrast, the submerged bed levels z_1 interpolated by Eq. 3 become lower with increasing distance from water edge.

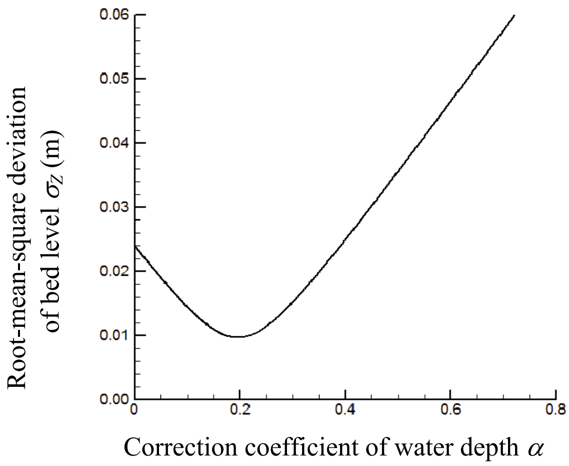

Figure 4 Error tendency of bed level with correction coefficient of water depth α

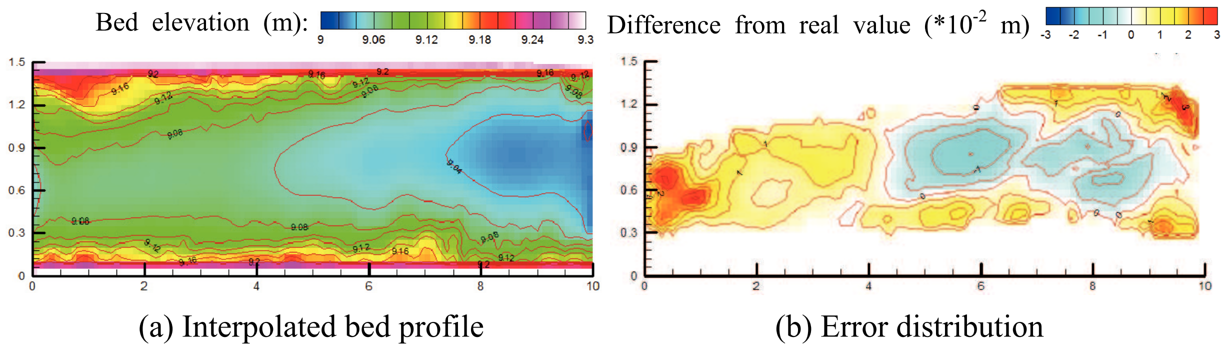

Figure 5 Interpolated bed profile and error distribution by geometry interpolated method of Eq. 1 with α=0.2

Figure 4 shows the error tendency of submerged bed level with constant correction coefficient of water depth α. Figure 5 (a) and (b) are the interpolated bed profile and the error distribution by the geometry interpolated method of Eq. 1 with the most probable value of constant α =0.2. The interpolated bed profile with α =0.2 captures the characteristics of the real profile of Figure 1. However, the root-mean-square deviation of bed level σ_Z cannot become zero for the constant value of α. This paper proposes how to determine the most probable value of α or its distribution dynamically by using water surface profile which can be obtain by bed level data at water edge.

3. HYDRODYNAMIC INTERPOLATION METHOD FOR SUBMERGED RIVER BED TOPOGRAPHY BY WATER SURFACE PROFILE

Numerical model for flow

The two-dimensional model (Uchida, 2006) is applied to simulation of water surface profiles of flows over undulating grounds for the hydrodynamic interpolation. The governing equations are continuity equation 5 and momentum equations 6:

$$\frac{\partial h}{\partial t} + \frac{1}{\lambda}\frac{\partial \lambda u_j h}{\partial x_j} = 0 \qquad (5)$$

$$\frac{1}{\lambda h}\left(\lambda\frac{\partial u_i h}{\partial t}+\frac{\partial \lambda u_i u_j h}{\partial x_j}\right) = -g\frac{\partial \zeta}{\partial x_i}-f_i+\frac{1}{\lambda h}\frac{\partial \lambda h\tau_{ij}}{\partial x_j} \quad (6)$$

where, subscripts i,j follow the summation convention, indicating 1=x and 2=y, respectively; h=water depth; u_i =velocity along x_i direction; λ=occupancy ratio of fluid; g=acceleration due to gravity; ζ=water surface elevation (h+z); z=ground elevation; f_i =external force except gravity; and τ_{ij} =horizontal shear stress tensors due to molecular and turbulent motions of fluids. Although the occupancy ratio of fluid γ is adopted in governing equations to capture complex shapes of boundaries (Uchida, 2006), γ=1 at every point in this study. f_i , which indicates bed shear stress in this study, is expressed by the logarithmic law with the equivalent sand roughness k_s as follows:

$$f_i=\tau_{0i}=C^2u_i\sqrt{u_j^{\,2}},\quad 1/C^2=\frac{1}{\kappa}(\ln\frac{h}{k_s}-1)+8.5 \quad (7)$$

The Reynolds stresses are represented by the Kinematic Eddy-Viscosity coefficient ν_t:

$$\tau_{ij}=\frac{\nu+\nu_t}{2}\left(\frac{\partial u_i}{\partial x_j}+\frac{\partial u_j}{\partial x_i}\right) \quad (8)$$

$$\nu_t=\frac{1}{6}\kappa u_* h \quad (9)$$

where κ=0.4, Karman's constant, u_*= friction velocity.

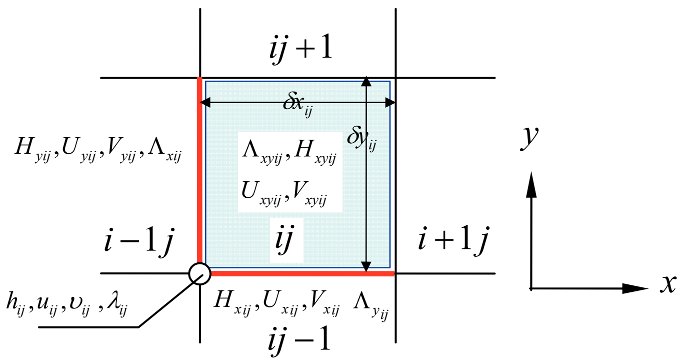

Figure 6 The arrangements of main variables on the computational control volume ij

The important points of the scheme are as follows (Uchida, 2006). For many numerical methods, interpolating algorisms are required to evaluate variables at several points of a control volume, which diminishes the computational accuracy and complicates the computational algorism. In this study, however, to directly capture the effect of distributed parameters in the Cartesian coordinate system, each control volume ij has three kinds of variables, i.e., the value at the intersection of the grid (Point Value, denoted by lower-case characters), the averaged value along the side of the grid (Line-averaged Value, denoted by capital letters with subscript of x or y) and the averaged value over the grid (Area-averaged Value, denoted by capital letters with subscript of xy). Those values are computed all together based on CIP-CSL scheme (Nakamura *et al.*, 2001). All the variables in the governing equations are set on the same location as shown in Figure 6. The interpolating operation of the variables is not necessary in the present scheme. Any boundary conditions can be taken into account without difficulty, because all the variables and parameters are well-defined in a computational cell based on the Control Volume Approach. The utilization of multi-valuables on a computational cell enables us not only to capture complex geometry even on the Cartesian coordinate system, but also to compute flow transitions with high resolution and accuracy. Details of numerical method and its performances are discussed in our previous paper (Uchida, 2006).

The boundary conditions of the flow computations are the experimental discharge given at the upstream end of the channel and the experimental water level at the downstream end. The computational grid sizes are dx=0.10 m, dy=0.05 m. For the practical case, we cannot prepare an appropriate value of the roughness coefficient of the submerged bed before the computation. In this paper, to simplify the problem, the equivalent sand roughness k_s=0.030 m is given for the computation of the bed shear stress by Eq. 7. Figure 7 shows longitudinal water level profiles at right and left water edges by measurement and computation with the real bed and k_s=0.030 m. The computed results are in good agreement with those of the measurement.

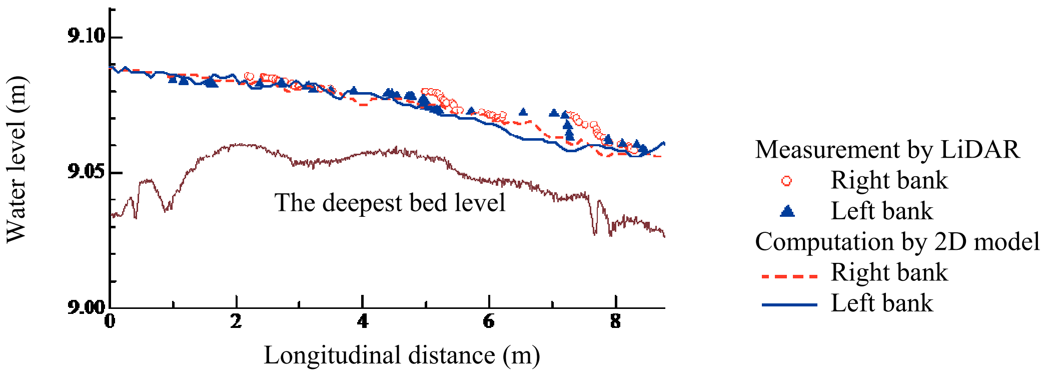

Figure 7 Longitudinal Water level profiles at water edge of right and left bank by the measurement and computation

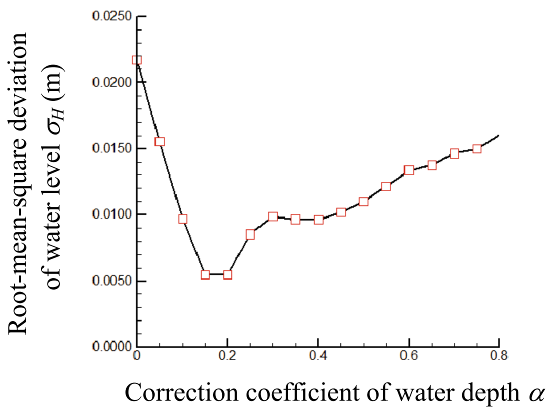

Figure 8 Error tendency of water level with correction coefficient of water depth α

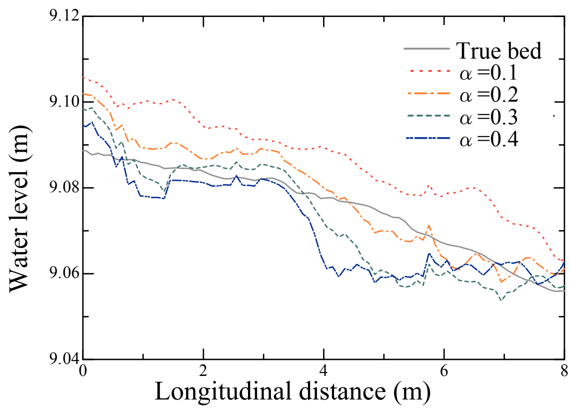

Figure 9 Computed water level profiles with various values of α

Error correlation between water surface and bed level profiles

To discuss the feasibility to interpolate river bed profile by known water surface profile, we conduct numerical simulations of flows for various bed topography (i.e., various value of α in Eq. 1) by the shallow water model, as shown in Figure 8. Figure 9 shows lateral averaged water level by the computations with various bed profiles. In this paper, true values of water levels are defined by the computed result with the true bed profile of Figure 7. The error tendency of the water level σ_H of Figure 8 is not simple as that of the ground level of Figure 4. The error tendency of the water level σ_H does not display a symmetrical pattern, in which there are extreme values at α=0.2 and 0.4, although the error tendency of the ground level σ_Z produces a symmetrical pattern with α=0.2 as an axis, as shown in Figure 4. This asymmetry is attributed to the constant downstream water level of the boundary condition. The error of ground level produces obvious error of water level, when the bed level is higher than that of true value. Conversely, the underestimated ground level does not produce the reveal error of water level. However, we can see that the least error of water surface leads to the least error of bed level. The above indicates that submerged river bed profiles can be interpolated by minimizing the error of water surface profiles.

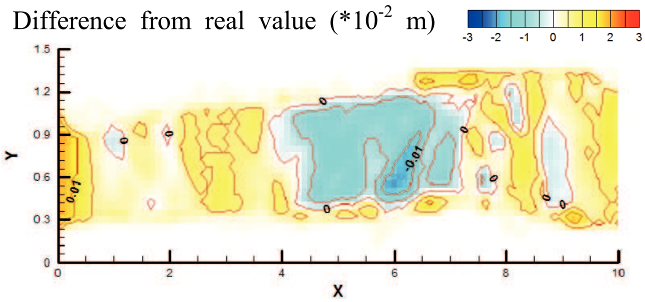

Figure 10 Error distribution of the water level computed with most probable value of α=0.2

Figure 10 shows the error distribution of water level computed with most probable value of α=0.2. The error distribution profile of the water level of Figure 10 is different from that of the bed level of Figure 5 (b). This indicates that it is difficult to estimate the submerged bed profiles (i.e., the distribution of α) directly by the error distribution of the water level.

Hydrodynamic interpolation method

Here, a new hydrodynamic interpolation method is developed to estimate the optimal submerged river bed topography using water surface profile. The base principle of the interpolation method is as follows. The proposition of this study can be defined " to obtain the bed elevation z_n at the submerged point n with the minimal square sum of difference of water level D_m^2 between measured and computed result". The gradient vector d_n is defined by the ratio of differential square sum of water level $\delta(D_m^2)$ to differential bed elevation δz_n:

$$d_n = (\delta D_m^{\ 2})_n / \delta z_n \tag{10}$$

The modifying bed elevation vector δz_n to decrease the square sum of difference of water level D_m^2 by a small value of βD_m^2 is described by Eq. 11 with use of the gradient vector d_n. Consequently, the proposition of this study can be redefined the nonlinear programming problem, in which the square sum of modified bed elevation vector δz_n^2 is minimised with constrained condition of Eq. (11) :

$$\text{constrained condition: } d_n \cdot \delta z_n = -\beta D_m^{\ 2} \tag{11}$$

$$\text{objective function: } \quad \delta z_n^{\ 2} \to \min \tag{12}$$

The optimized solution of the differential bed elevation δz_n, which decrease D_m^2 by βD_m^2 with its own minimal square sum δz_n^2, is obtained by Lagrange's method of undetermined multipliers, as Eq. 13.

$$\delta z_n = -\beta D_m^{\ 2} \cdot d_n / d_l^{\ 2} \tag{13}$$

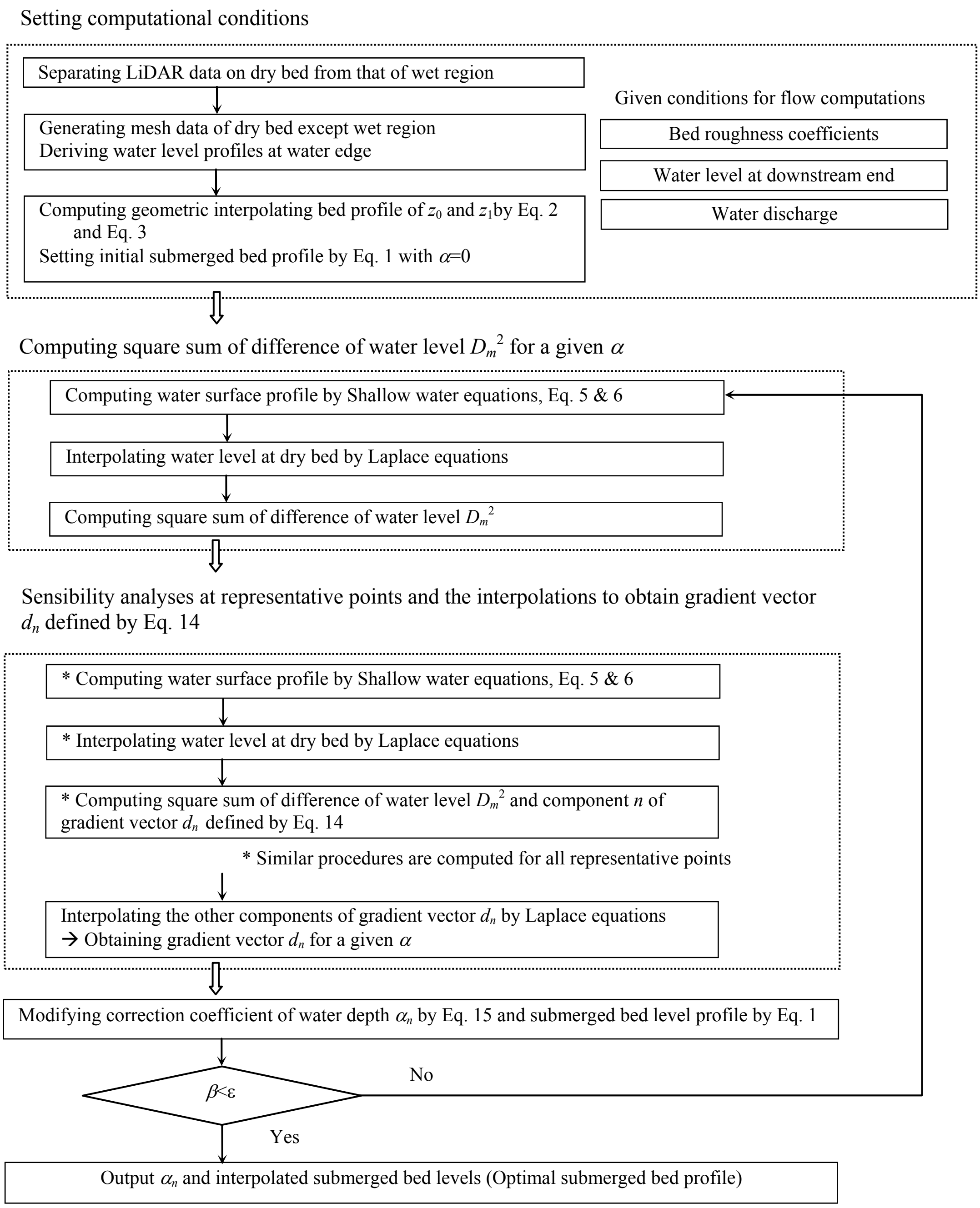

Figure 11 Computational procedures of the hydrodynamic interpolation method to obtain optimal submerged river bed topography using water surface profile

in which, d_l^2 is square sum of gradient vector d_n.

In this paper, the modifying vector of correction coefficient of water depth $\delta\alpha_n$ is computed instead of δz_n to reduce the computational load. The gradient vector d_n of differential square sum of water level $\delta(D_m^2)$ with respect to differential correction coefficient of water depth $\delta\alpha_n$:

$$d_n = (\delta D_m{}^2)_n \big/ \delta\alpha_n \tag{14}$$

The optimized solution of the differential correction coefficient of water depth $\delta\alpha_n$, which decrease D_m^2 by βD_m^2 with its own minimal square sum $\delta\alpha_n^2$, is obtained in the same manner as described above.

$$\delta\alpha_n = -\beta D_m{}^2 \cdot d_n / d_l{}^2 \qquad (15)$$

The optimal value of correction coefficient of water depth α_n is obtained by the following numerical integration of the differential correction coefficient of water depth $\delta\alpha_n$ with a small vale of β and the gradient vector d_n.

The gradient vector d_n is obtained by the sensibility analysis of the 2-D shallow water model indicated in the previous chapter. The sensibility analyses are conducted at representative points of submerged grids, and then the sensitivities at the other grids are interpolated by that of the representative points to reduce the computational load. Because the wet regions with half-interpolated submerged bed topography are different from the true wet region, virtual water levels at dry regions are interpolated by that of the wet regions, to compute square sum of difference of water level D_m^2. The above interpolations are computed by the Laplace equations.

Figure 11 shows the computational procedures of the hydrodynamic interpolation method for submerged river bed topography by water surface profile. The procedures are divided by setting computational conditions, computing square sum of difference of water level D_m^2 for a given α and sensibility analyses by the 2-D shallow water model to obtain gradient vector d_n. For setting computational conditions, in this study, computed water levels with the true bed topography measured by LiDAR are used instead of measured water level profiles at the water edges by LiDAR data. The initial values of α_n=0 are given at every submerged grids, in which zero water depth is assumed, because it is difficult to modify overvalued α to its appropriate value, as noticed by Figure 8. Consequently, the locally optimal solution of submerged bed topography with the minimum water depth is computed by the present method. To procedure this method properly, it is noticed by the assumption of Equation 11 that a small vale of β should be used. In this paper, β is given by the ratio of reduced value of ΔD_m^2 at a last computational step to D_m^2. The computation are continued until β becomes smaller than ε=10^{-3}.

Results and discussions

Figure 12 shows the root-mean-square deviation of water level σ_H with computational steps, and Figure 13 shows the distribution of the eventual water level deviation. Although, the eventual water level deviation does not become zero, the present method decrease the root-mean-square deviation of water level σ_H with computational step monotonically.

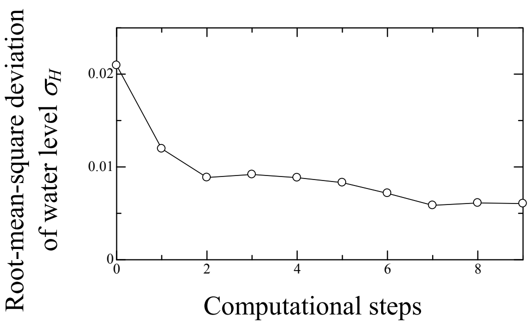

Figure 12 Root-mean-square deviation of water level σ_H with computational steps

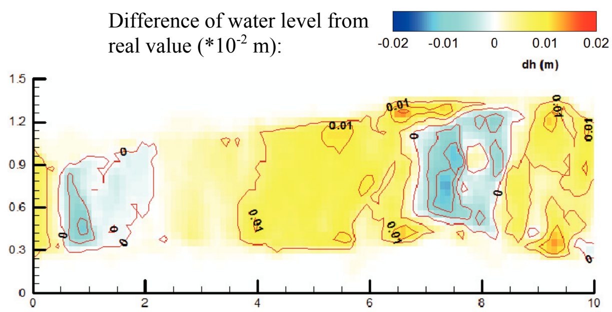

Figure 13 Error distribution of the eventual water level by the present method

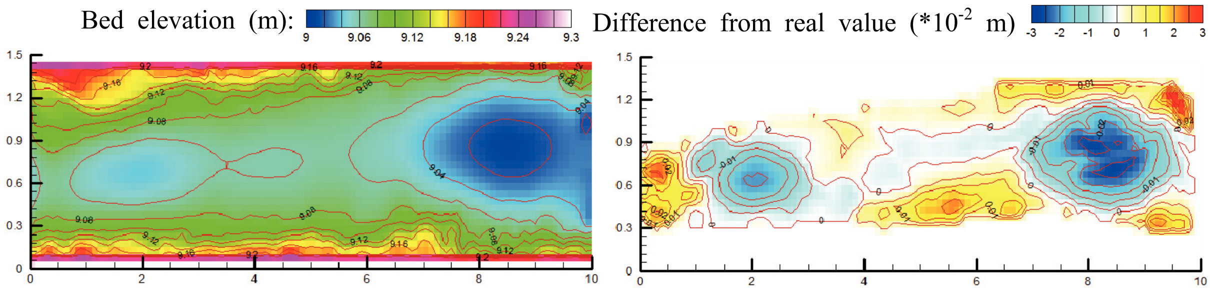

(a) Interpolated bed profile (b) Error distribution

Figure 14 The optimal solution of bed topography and error distribution by present hydrodynamic interpolated method of Fig. 11

Figure 14 shows the optimal solution of bed topography and the distribution of the deviation of the eventual bed level deviation. The eventual submerged bed topography still remains the deference from the real value as well as the water surface. However, the difference between the eventual and the actual bed levels are very small. So, it is significant results that the submerged bed shape can be hydrodynamically interpolated by reproducing water surface profiles by present model in compensation for the weak point of LiDAR.

CONCLUSIONS

Numerical simulations of flows for various bed topographies by the shallow water model are conducted to discuss the feasibility to interpolate river bed profile from known water surface profile. The results show that the least error of water surface leads to the least error of submerged bed to topography. The above indicates that submerged river bed profiles can be interpolated by minimizing the error of water surface profiles. The error of ground level produces obvious error of water level, when the bed level is higher than that of true value. Conversely, the underestimated ground level does not produce the reveal error of water level.

This paper proposes a new hydrodynamic interpolation method, in which the locally optimal solution of submerged bed topography with the minimum water depth is computed. It is confirmed that the present method can modify the submerged bed toward the measured one. Because longitudinal water level profiles can be obtained by LiDAR, the present method may be a powerful technique to interpolate the submerged bed topography in compensation for the weak point of LiDAR.

REFERENCES

Nakamura, T., Tanaka, R., Yabe, T., and Takizawa, K. (2001) Exactly conservative semi-Lagrangian scheme for multi-dimensional hyperbolic equations with directional splitting technique, *Journal of Computational Physics* 174, pp. 171-207.

Uchida, T. (2006) A CIP-based method for shallow water flows in complex geometries using Cartesian grids, *Proceedings of 7th International Conference on Hydroscience and Engineering, ICHE-2006*, Philadelphia, 2006.9.

Uchida, T., Kawahara, Y., Yamamizu, R., Watanabe, Y. and Moriyama, M. (2007) Measurement of physical surroundings of river with a helicopter-mounted 3D Laser Scanner System of high precision, *Advanced in River Engineering*, *JSCE*, Vol.13, pp.243-248, in Japanese.